Chinese Journal of Natural Medicines

Neferine sensitizes oral squamous cell carcinoma to cisplatin by disrupting the CCDC43–PNKP interaction

Yangfeng Lin, Xiongzhou Zheng, Yue Tang, Jianguang Chen, Xiao Chen, Zixi Liang, Xian Lin, Xiaofeng Zhu

Citation: Yangfeng Lin, Xiongzhou Zheng, Yue Tang, Jianguang Chen, Xiao Chen, Zixi Liang, Xian Lin, Xiaofeng Zhu, Neferine sensitizes oral squamous cell carcinoma to cisplatin by disrupting the CCDC43–PNKP interaction, Chinese Journal of Natural Medicines, 2026, 24(11), 1343–1353. doi: 10.1016/S1875–5364(26)61224–1.

View online: https://doi.org/10.1016/S1875–5364(26)61224–1

Related articles that may interest you

Gambogenic acid induces apoptosis *via* upregulation of Noxa in oral squamous cell carcinoma

Chinese Journal of Natural Medicines. 2024, 22(7), 632–642 https://doi.org/10.1016/S1875–5364(24)60578–9

Probing the new strategy for the oral formulations of taxanes: changing the method with the situation

Chinese Journal of Natural Medicines. 2021, 19(9), 656–665 https://doi.org/10.1016/S1875–5364(21)60096–1

Hernandezine promotes cancer cell apoptosis and disrupts the lysosomal acidic environment and cathepsin D maturation

Chinese Journal of Natural Medicines. 2024, 22(5), 387–401 https://doi.org/10.1016/S1875–5364(24)60638–2

Transcriptome sequencing and metabolome analysis reveal the mechanism of Shuanghua Baihe Tablet in the treatment of oral mucositis

Chinese Journal of Natural Medicines. 2021, 19(12), 930–943 https://doi.org/10.1016/S1875–5364(22)60150–X

Maackiain inhibits proliferation and promotes apoptosis of nasopharyngeal carcinoma cells by inhibiting the MAPK/Ras signaling pathway

Chinese Journal of Natural Medicines. 2023, 21(3), 185–196 https://doi.org/10.1016/S1875–5364(23)60420–0

Jinyinqingre Oral Liquid alleviates LPS–induced acute lung injury by inhibiting the NF–κB/NLRP3/GSDMD pathway

Chinese Journal of Natural Medicines. 2023, 21(6), 423–435 https://doi.org/10.1016/S1875–5364(23)60397–8

Wechat

Chinese Journal of Natural Medicines 24 (2026) 1343-1353

Contents lists available at ScienceDirect

Chinese Journal of Natural Medicines

journal homepage: www.cjnmcpu.com/



Original article

Neferine sensitizes oral squamous cell carcinoma to cisplatin by disrupting the CCDC43-PNKP interaction

Yangfeng Lin[a,Δ], Xiongzhou Zheng[b,Δ], Yue Tang[c,d,Δ], Jianguang Chen[b,Δ], Xiao Chen[e,f,Δ], Zixi Liang[g], Xian Lin[h,i,j,*], Xiaofeng Zhu[c, d,*]

[a] *Department of Oncology Surgery II, The First Hospital of Putian City, Putian 351100, China*
[b] *Department of otorhinolaryngology, Xianyou County General Hospital, Xianyou 351200, China*
[c] *Department of Oral Maxillo-Facial Surgery, The First Affiliated Hospital, Fujian Medical University, Fuzhou 350005, China*
[d] *Department of Oral Maxillo-Facial Surgery, National Regional Medical Center, Binhai Campus of the First Affiliated Hospital, Fujian Medical University, Fuzhou 350212, China*
[e] *Department of Intensive Care Unit, The First Affiliated Hospital, Fujian Medical University, Fuzhou 350005, China*
[f] *Department of Intensive Care Unit, National Regional Medical Center, Binhai Campus of the First Affiliated Hospital, Fujian Medical University, Fuzhou 350212, China*
[g] *Department of Gastroenterology, Third Affiliated Hospital of Sun Yat-Sen University, Guangzhou 510620, China*
[h] *Shengli Clinical Medical College of Fujian Medical University, Fujian Provincial Hospital, Fuzhou University Affiliated Provincial Hospital, Fuzhou 350001, China*
[i] *Key Laboratory of Radiation Biology of Fujian higher education institutions, The First Affiliated Hospital, Fujian Medical University, Fuzhou 350005, China*
[j] *Shenzhen Key Laboratory of Inflammatory and Immunology Diseases, Shenzhen 518036, China*

ARTICLE INFO

Article history:
Received 21 February 2026
Revised 12 April 2026
Accepted 16 June 2026
Available online 20 November 2026

Keywords:
Neferine
CCDC43
PNKP
Oral cancer
Chemosensitivity

ABSTRACT

Oral squamous cell carcinoma (OSCC) poses a significant global health challenge due to its high recurrence rate and resistance to cisplatin. While DNA repair pathways contribute to chemoresistance, the role of scaffold proteins in stabilizing repair enzymes remains largely unexplored. This study aimed to elucidate the function of CCDC43 in cisplatin sensitivity and to identify a natural product targeting the CCDC43-PNKP axis. Bioinformatic analyses were conducted using bulk and single-cell transcriptomic and proteomic datasets. Molecular assays investigated the CCDC43-PNKP interaction and the impact of neferine on this axis. Xenograft models assessed the efficacy of combined neferine and cisplatin treatment. Machine learning identified CCDC43 as a key prognostic marker and driver of cisplatin resistance. CCDC43 was upregulated in OSCC epithelial cells and associated with poor survival. CCDC43 bound and stabilized PNKP by inhibiting ubiquitin-dependent degradation, thereby enhancing DNA repair and reducing cisplatin sensitivity. Through artificial intelligence-based virtual screening and experimental validation, neferine was found to disrupt the CCDC43-PNKP interaction, promoted PNKP degradation, increased cisplatin-induced DNA damage, and suppressed OSCC growth without acute toxicity. Collectively, the CCDC43-PNKP axis represents a critical therapeutic target in OSCC. Neferine is a promising ethnopharmacological agent capable of improving cisplatin sensitivity by targeting this pathway.

1. Introduction

Oral squamous cell carcinoma (OSCC) is a major global health burden, accounting for the vast majority of head and neck cancers [1, 2]. Despite advancements in surgical techniques and radiotherapy, the five-year survival rate for patients with advanced OSCC remains alarmingly low [3]. This stagnation is primarily attributed to high rates of local recurrence and, most critically, the development of resistance to systemic chemotherapy [4]. Therefore, overcoming chemoresistance in OSCC has important clinical implications.

Cisplatin (CDDP) remains the first-line chemotherapeutic agent for OSCC. Its mechanism of action involves the formation of platinum-DNA adducts, primarily intra-strand and inter-strand crosslinks. These lesions distort the DNA double helix and block the progression of RNA polymerase and DNA polymerase, thereby triggering cell cycle arrest [5]. However, the efficacy of cisplatin is frequently compromised by the adaptive activation of the DNA repair signaling [6, 7]. Furthermore, the clinical use of cisplatin is limited by severe systemic toxicities. Therefore, a high priority in ethnopharmacological research is to identify natural compounds that synergize with cisplatin, enabling dose reduction while maintaining efficacy. Neferine, a bioactive bisbenzylisoquinoline alkaloid derived from the green embryos of *Nelumbo nucifera* Gaertn. (known as Lian Zi Xin in Traditional Chinese Medicine), has been used for centuries to treat conditions associated with "heat-toxin", a traditional concept that encompasses inflammation, hyperproliferation, and recalcitrant pathological states [8]. In modern pharmacological terms, neferine has demonstrated multi-targeted anticancer effects, including chemosensitization to other anticancer drugs [9]. However, whether neferine modulates DNA repair to affect chemosensitivity remains unknown.

* Corresponding author.
E-mail addresses: linxiangabriel@fjmu.edu.cn (X. Lin); zhuxiaofengfjmu@163.com; dentzxf@163.com (XF. Zhu)
Δ These authors contributed equally to this work.

https://doi.org/10.1016/S1875-5364(26)61224-1
Copyright © 2026, China Pharmaceutical University. Published by Elsevier B.V. All rights are reserved.

Cancer cells evolve to overexpress specific DNA repair enzymes that can efficiently excise or bypass platinum-induced lesions [10]. Among the various repair pathways, base excision repair and non-homologous end joining are paramount in resolving the types of damage caused by cisplatin [11]. A central enzyme in these pathways is PNKP, which is a unique bifunctional enzyme that restores DNA termini to a 3'-hydroxyl and 5'-phosphate configuration, a prerequisite for ligation by DNA ligases [12]. Elevated PNKP activity has been linked to radio- and chemoresistance in several solid tumors [13, 14], yet the factors that regulate its protein stability and recruitment in OSCC remain poorly defined .

Scaffold proteins, particularly those containing coiled-coil domains, have emerged as essential regulators of the DNA damage response [15]. These proteins do not possess intrinsic enzymatic activity but serve as molecular "glue" or platforms that bring together repair enzymes and their substrates [16]. CCDC43 is a relatively understudied member of the CCDC family [17]. Although initial reports have implicated it in apoptosis as well as cancer proliferation and metastasis [18-20], its role in DNA repair and chemosensitivity in OSCC has not been elucidated.

Our preliminary studies demonstrated the anticancer properties of multiple natural compounds [21-23]. In this study, we integrated machine learning-based target discovery with multi-omics analysis to identify CCDC43 as a potential cancer driver in OSCC and investigated its role in DNA repair and chemosensitivity. Using artificial intelligence-based virtual screening (AI-based VS), we identified neferine as a potential inhibitor of CCDC43-PNKP protein-protein interaction (PPI) and validated its therapeutic effect in OSCC. The effect of neferine on CCDC43-mediated cisplatin sensitivity was detected to evaluate CCDC43 as a therapeutic target and neferine as a natural drug candidate for OSCC.

2. Materials and methods

2.1. Bioinformatics and machine learning pipeline

To identify high-confidence prognostic markers for OSCC, we retrieved transcriptomic and clinical data for head and neck squamous cell carcinoma (HNSCC) patients from The Cancer Genome Atlas (TCGA), multiple Gene Expression Omnibus (GEO) datasets (GSE42743, GSE41613, GSE65858, GSE75538, and GSE117973), and the EMBL-EBI ArrayExpress repository (E-MTAB-8588). Proteomic and clinical data for HNSC were sourced from clinical proteomic tumor analysis consortium (CPTAC) and the Human Protein Atlas. Feature selection was performed using three complementary machine learning algorithms. First, Random Forest analysis was implemented with the randomForest R package using 1000 trees, and feature importance was ranked by the Mean Decrease Gini index to identify genes most predictive of tumor versus normal status and survival outcomes. Second, support vector machine-recursive feature elimination (SVM-RFE) was applied using the e1071 R package to determine the optimal feature subset for classification. Third, least absolute shrinkage and selection operator (LASSO) regression was performed with 10-fold cross-validation using the glmnet R package. Genes commonly identified by all three algorithms were selected for subsequent validation. Gene set enrichment analysis (GSEA) and hallmark pathway analysis were conducted to investigate the biological functions and signaling pathways associated with CCDC43 expression.

2.2. Single-cell RNA sequencing (scRNA-seq) analysis

Raw single-cell RNA sequencing data from OSCC patients (GSE172577 and GSE181919) were processed using the Seurat pipeline. Cells with fewer than 200 or more than 6000 detected genes, or with >15% mitochondrial gene content, were excluded. Data were normalized using the SCTransform method. Dimensionality reduction was performed *via* principal component analysis (PCA) and uniform manifold approximation and projection (UMAP). Cell types were annotated based on canonical marker genes. CCDC43 expression was visualized using FeaturePlot and VlnPlot functions.

2.3. Cell culture and chemical agents

The human OSCC cell lines CAL27 and SCC25 were purchased from Procell Corporation (Wuhan, China) and cultured in DMEM/F12 supplemented with 10% heat-inactivated fetal bovine serum. Neferine (purity ≥ 99%) and cisplatin (purity ≥ 99%) were obtained from TargetMol Biotechnology (Boston, MA, USA). Stock solutions were prepared by dissolving neferine in DMSO and cisplatin in H_2O.

2.4. Cell transduction and transfection

Lentiviral particles encoding short hairpin RNA (shRNA) targeting CCDC43 were purchased from GeneChem Inc. (Shanghai, China). For overexpression, CCDC43 plasmids were obtained from Vigene Biosciences (Shandong, China). Knockdown was achieved by lentiviral transduction in the presence of polybrene, while plasmid transfection was performed using Lipofectamine™ 3000 (Invitrogen, Shanghai, China). Knockdown and overexpression efficiencies were confirmed by reverse transcription quantitative polymerase chain reaction (RT-qPCR) and western blot.

2.5. RT-qPCR

Total RNA was extracted from OSCC cells and reverse-transcribed into cDNA. The resulting cDNA was then amplified by qPCR using specific primers (Table S1). Relative mRNA expression levels were calculated using the $2^{-\Delta\Delta Ct}$ method.

2.6. Western blot

OSCC cells were collected and lysed for protein extraction. Protein concentrations were determined using a BCA assay. Equal amounts of protein were separated by SDS-PAGE, transferred to PVDF membranes, and immunoblotted with specific antibodies (Table S2). Protein signals were visualized using an enhanced chemiluminescence detection.

2.7. Colony formation assay

For the colony formation assay, OSCC cells were seeded in 6-well plates at 500 cells per well and cultured for 14 days, with medium replacement every 3 days. Colonies were then fixed with methanol for 20 min, stained with 0.5% crystal violet for 30 min, washed with distilled water, and air-dried overnight. Colonies containing > 50 cells were counted under a light microscope.

2.8. Immunofluorescence

OSCC cells were seeded on 96-well plates, cultured, and then fixed with 4% paraformaldehyde. After permeabilization with 0.2% Triton X-100, cells were incubated with primary antibodies (Table S2), followed by staining with DAPI (0.2 μg·mL^{-1}). Images were captured using a fluorescence microscope.

2.9. EdU incorporation assays

EdU incorporation was assessed using the Apollo567 in vitro imaging kit (RiboBio, Guangzhou, China) according to the manufacturer's instructions. OSCC cells were treated with 10 μmol·L^{-1}

EdU for 2 h, then fixed with 4% paraformaldehyde, permeabilized with 0.2% Triton X-100, and stained with Apollo fluorescent dye and DAPI (5 μg·mL^{-1}). EdU-positive cells were visualized and quantified under a fluorescence microscope.

2.10. CCK-8 assay

OSCC cells were seeded in 96-well plates and treated with increasing concentrations of neferine (0, 2, 5, 10, 20, 50, and 100 μmol·L^{-1}) or cisplatin (0, 2.5, 5, 10, 20, and 40 μmol·L^{-1}). Subsequently, 10 μL of CCK-8 reagent was added to each well and incubated for 1 h. Absorbance was measured at 450 nm using a Synergy™ H1 Multimode Reader (BioTek, USA).

2.11. Co-Immunoprecipitation (Co-IP)

Co-IP assays were performed using a Pierce Co-IP kit (Thermo Fisher Scientific) as previously described [24]. Briefly, OSCC cells were lysed, and protein concentrations were determined by BCA assay. For immunoprecipitation, 5 mg of total protein was incubated overnight with 10 μg of target-specific antibody or control IgG (Table S2). Immunocomplexes were then eluted and analyzed by western blot.

2.12. Cycloheximide (CHX) chase assays

To assess protein stability, CHX chase assays were performed as described previously [7]. OSCC cells were treated with 50 μg·mL^{-1} CHX and harvested at the indicated times. Protein lysates were prepared, quantified by BCA assay, and analyzed by western blot to monitor protein degradation kinetics.

2.13. Protein-protein docking, AI-based VS, and molecular docking

The three-dimensional structures of CCDC43 and PNKP, predicted by AlphaFold, were downloaded from the UniProt database. Protein-protein docking was carried out using the GRAMM-X web server, and the putative binding interface was visualized and analyzed with PDBePISA. Virtual screening was conducted using the HelixVS platform (https://paddlehelix.baidu.com/app/drug/helixvs/forecast), a deep learning-enhanced structure-based virtual screening tool. The binding pocket was defined as the PNKP interface involved in the CCDC43-PNKP interaction, as predicted by GRAMM-X protein-protein docking. The TargetMol Natural Product Library (Catalog No. L6020, n = 19 377) was screened using default parameters. The platform automatically executed a three-stage pipeline: (1) rapid docking with AutoDock QuickVina 2 to generate candidate conformations; (2) deep learning-based re-scoring using the RTMScore architecture to evaluate binding affinities; and (3) conformational filtering and clustering based on predefined binding mode criteria. The top-ranked compounds were selected for experimental validation. To further characterize the interaction, molecular docking were performed using the CB-Dock2 AI-driven platform, with binding affinities evaluated based on Vina scores.

2.14. Cellular thermal shift assay (CETSA)

CETSA was performed as previously described [25]. Briefly, OSCC cells treated with or without neferine were harvested and lysed. Lysates were clarified by centrifugation, diluted in buffer containing protease inhibitors, and aliquoted (30 μL per sample). Each aliquot was heated at indicated temperatures (40, 43, 46, 49, 52, 55, 58, and 61 °C) for 3 min, followed by 3 min incubation at room temperature. Heated lysates were then centrifuged, and the supernatants were collected for western blot analysis.

2.15. In vivo xenograft model

Animal studies were approved by the Institutional Animal Care and Use Committee (No. 2024-632). CAL27 cells (5 × 10^6) were injected subcutaneously into male BALB/c nude mice (4–5 weeks old). Once tumor volume reached approximately 100 mm^3, mice were randomly divided into three groups (n = 5 per group) and treated with: (1) saline (control), (2) cisplatin (5 mg·kg^{-1}, i.p., twice weekly), or (3) neferine (10 mg·kg^{-1}, i.p., daily) combined with cisplatin (5 mg·kg^{-1}, i.p., twice weekly). At the endpoint, mice were euthanized, and tumors were excised and weighed. To assess *in vivo* toxicity, separate cohorts received neferine (10 mg·kg^{-1}) or saline via intraperitoneal injection. For acute toxicity assessment, separate cohorts of C57BL/6 mice (6–8 weeks old) received neferine (10 mg·kg^{-1}, i.p., daily) or an equal volume of saline for 14 consecutive days. Serum samples were collected for measurement of alanine aminotransferase (ALT), aspartate aminotransferase (AST), blood urea nitrogen (BUN), and creatinine (CREA) using an automated analyzer. Major organs (liver and kidney) were harvested, fixed in 4% paraformaldehyde, and processed for H&E staining to evaluate histopathological changes.

2.16. Immunohistochemistry

Paraffin-embedded tissue sections (4 μm) were deparaffinized, rehydrated, and subjected to antigen retrieval in citrate buffer. Endogenous peroxidase activity was blocked with 3% H_2O_2, and non-specific binding was blocked with goat serum. Sections were then incubated with primary antibodies (Table S2), and signals were visualized using a DAB substrate kit (Maixin Biotech., Fuzhou, China).

2.17. Statistical analysis

Statistical analysis was performed using SPSS (version 22.0) and R (version 4.4.1). Results from three independent experiments were expressed as mean ± standard deviation. Differences between two groups were assessed using two-tailed Student's t-test, and comparisons among multiple groups were analyzed by one-way ANOVA with Tukey's HSD post-hoc test. A P-value < 0.05 was considered statistically significant.

3. Results

3.1. Machine learning identified CCDC43 as a prognostic predictor in OSCC

To systematically identify genes driving OSCC progression, we employed three independent machine learning algorithms on the TCGA-HNSC dataset. Random Forest analysis identified CCDC43 as a gene with a high Mean Decrease Gini score, indicating its importance in distinguishing tumor from normal tissue and predicting patient survival (Figs. 1A–1D). SVM-RFE further narrowed the gene list, showing that CCDC43 was a critical feature for high-accuracy classification (Figs. 1E and 1F). Finally, LASSO regression confirmed CCDC43 as a key gene capable of distinguishing tumor from normal tissue and predicting patient survival (Figs. 1G and 1H). Among the top three intersecting genes, CCDC43 ranked first.

Validation across multiple bulk transcriptomic cohorts (TCGA, GSE42743) revealed that CCDC43 mRNA was significantly upregulated in OSCC compared to adjacent normal tissues (Fig. 2A). Clinically, high CCDC43 levels correlated with advanced T-stage (Fig. 2B), positive lymph node metastasis (N-stage, Fig. 2C), and pathological grade (Fig. 2D). Most importantly, COX regression analysis and Kaplan-Meier survival curves demon-

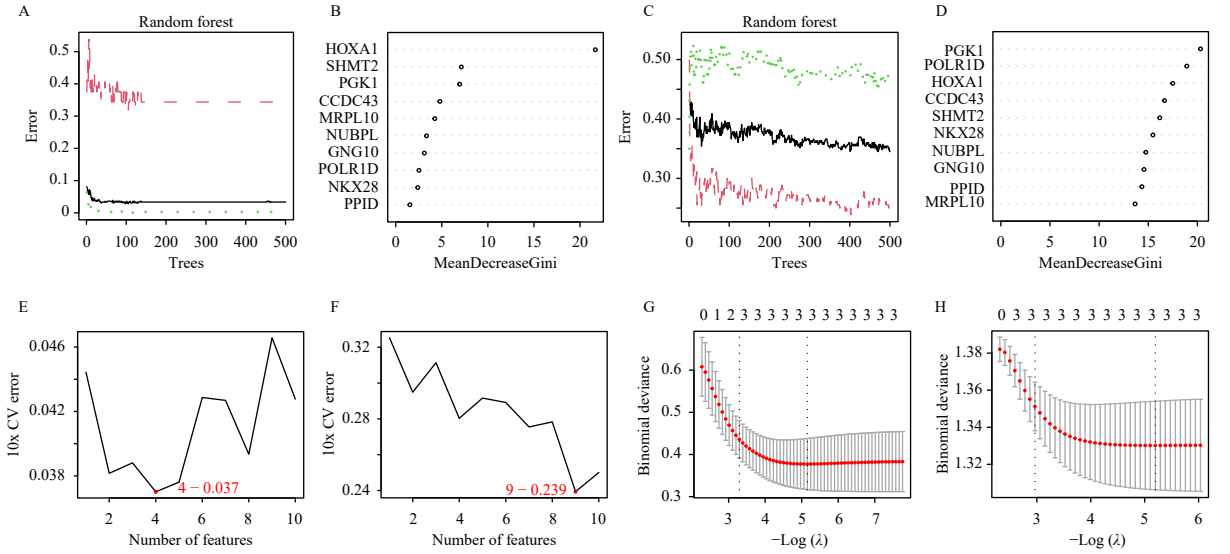


Fig. 1 Identification of OSCC- and survival-associated genes using machine learning in TCGA. (A-D) Genes associated with OSCC (A, B) and patient survival (C, D) were ranked by Random Forest analysis. (E, F) SVM-RFE identified genes associated with OSCC (E) and patient survival (F). (G, H) LASSO regression recognized genes associated with OSCC (G) and patient survival (H).

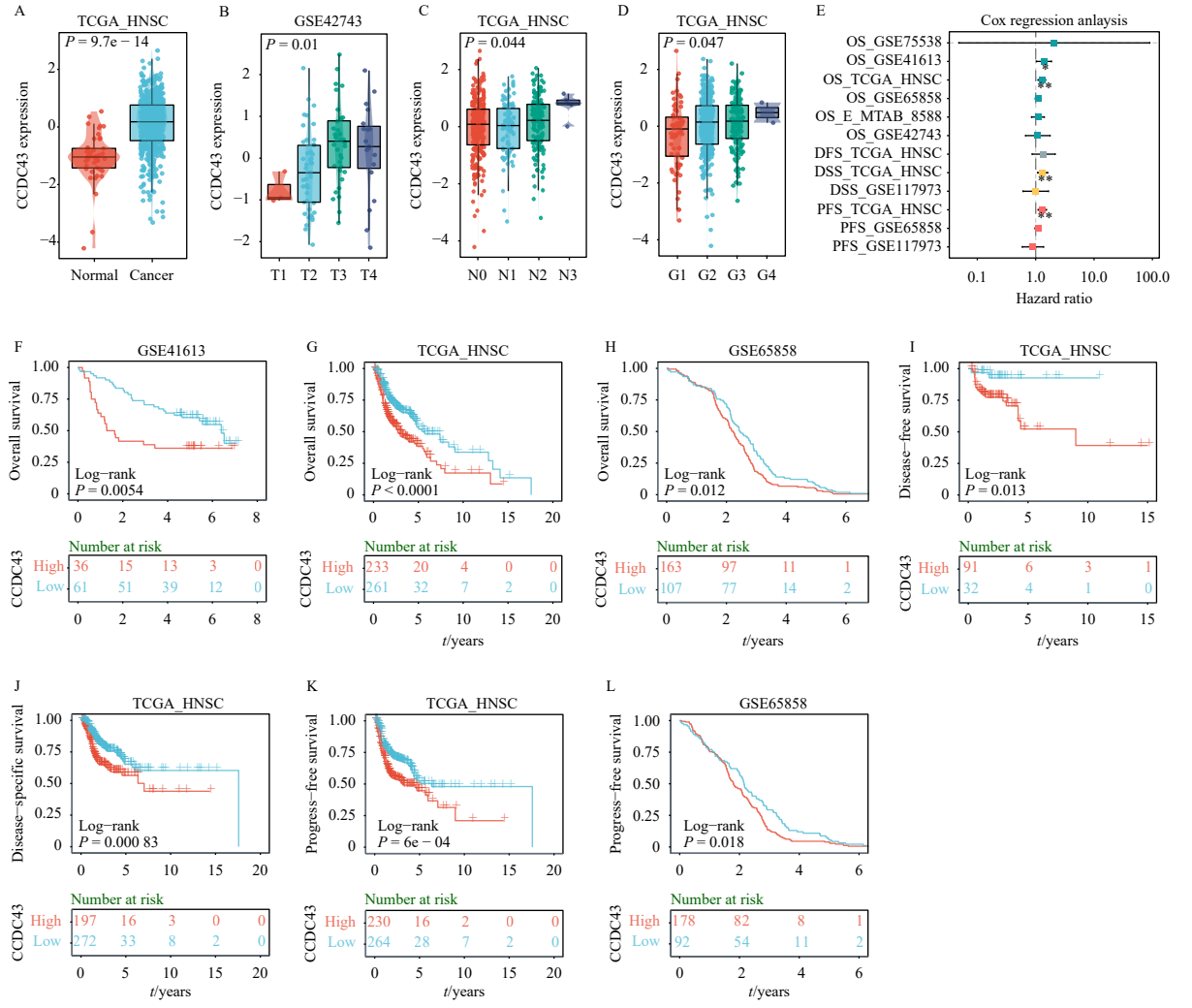


Fig. 2 CCDC43 expression and clinical relevance in HNSC datasets revealed by bulk transcriptomics. (A) CCDC43 expression was upregulated in tumor tissues compared to normal controls in TCGA_HNSC. (B) Positive correlation between CCDC43 expression and T stage in GSE42743. (C) Positive correlation between CCDC43 expression and N stage in TCGA_HNSC. (D) Positive correlation between CCDC43 expression and pathological stage in TCGA_HNSC. (E) CCDC43 expression correlated with poor prognosis across multiple HNSC datasets. (F–H) High CCDC43 expression correlated with shorter OS in GSE41613 (F), TCGA_HNSC (G), and GSE65858. (I) High CCDC43 expression correlated with shorter DFS in TCGA_HNSC. (J) High CCDC43 expression correlated with shorter DSS in TCGA_HNSC. (K, L) High CCDC43 expression correlated with shorter PFS in TCGA_HNSC and GSE65858. * $P < 0.05$ and ** $P < 0.01$ *vs* the CCDC43 low-expression group.

strated that patients with high CCDC43 expression had significantly shorter overall survival (OS), disease-free survival (DFS), disease-specific survival (DSS), and progression-free survival (PFS) across the TCGA, GSE41613, and GSE65858 datasets (Figs. 2E–2L), suggesting CCDC43 as a prognostic driver.

3.2. CCDC43 was specifically enriched in malignant epithelial cells of OSCC

We further validated these findings at the protein level using the CPTAC proteomic dataset. CCDC43 protein expression was significantly upregulated in HNSCC samples relative to normal tissues (Fig. 3A, Table S3) and were predictive of poor OS (Fig. 3B). Immunohistochemical staining from the Human Protein Atlas confirmed strong cytoplasmic and nuclear CCDC43 expression in OSCC sections, while normal oral mucosa showed minimal staining (Fig. 3C).

To pinpoint the cellular source of CCDC43 within the complex tumor microenvironment, we analyzed scRNA-seq data from two independent cohorts (GSE172577 and GSE181919). After clustering and cell-type annotation, we found that CCDC43 expression was almost exclusively restricted to the tumor epithelial cell cluster (Figs. 3D–3I). This cell-type specificity suggested that CCDC43 exerted a cell-intrinsic oncogenic function.

3.3. CCDC43 was linked to DNA repair and platinum resistance

GSEA was performed to explore the biological pathways associated with CCDC43. High CCDC43 expression was significantly enriched in KEGG pathways related to DNA damage repair and DNA replication (Fig. 4A). Similarly, HALLMARK analysis showed a strong correlation with the DNA repair signaling (Fig. 4B).

Given these findings, we investigated the relationship between CCDC43 and platinum sensitivity. Using the cancer therapeutics response portal database (https://portals.broadinstitute.org/ctrp/), we observed that OSCC cell lines with high CCDC43 expression exhibited significantly higher IC50 values for platinum (Fig. 4C). This positive correlation between CCDC43 expression and platinum IC50 was consistently observed in the GSE41613, GSE42743, and TCGA cohorts (Figs. 4D–4F), strongly suggesting that CCDC43 contributed to chemoresistance.

3.4. CCDC43 depletion impaired DNA repair and sensitized OSCC cells to platinum

To confirm the functional role of CCDC43, we established stable CCDC43-knockdown CAL27 and SCC25 cell lines (Figs. 5A–5C). Silencing CCDC43 significantly reduced the colony-forming capacity of OSCC cells and markedly sensitized them to cisplatin (Figs. 5D and 5E). Moreover, CCK-8 assays revealed that CCDC43 knockdown enhanced cisplatin sensitivity (Figs. S1A and B). To determine if this sensitization was due to defective DNA repair, we monitored γ-H2AX foci, a marker for DNA damage. While cisplatin induced a baseline level of γ-H2AX, CCDC43 knockdown led to a dramatic and persistent accumulation of γ-H2AX foci following cisplatin treatment (Figs. 5F–5I). Furthermore, EdU incorporation assays showed that silencing CCDC43 enhanced the inhibitory effect of cisplatin on DNA replication (Figs. 5J–5M). Collectively, these findings indicated that CCDC43 reduced platinum

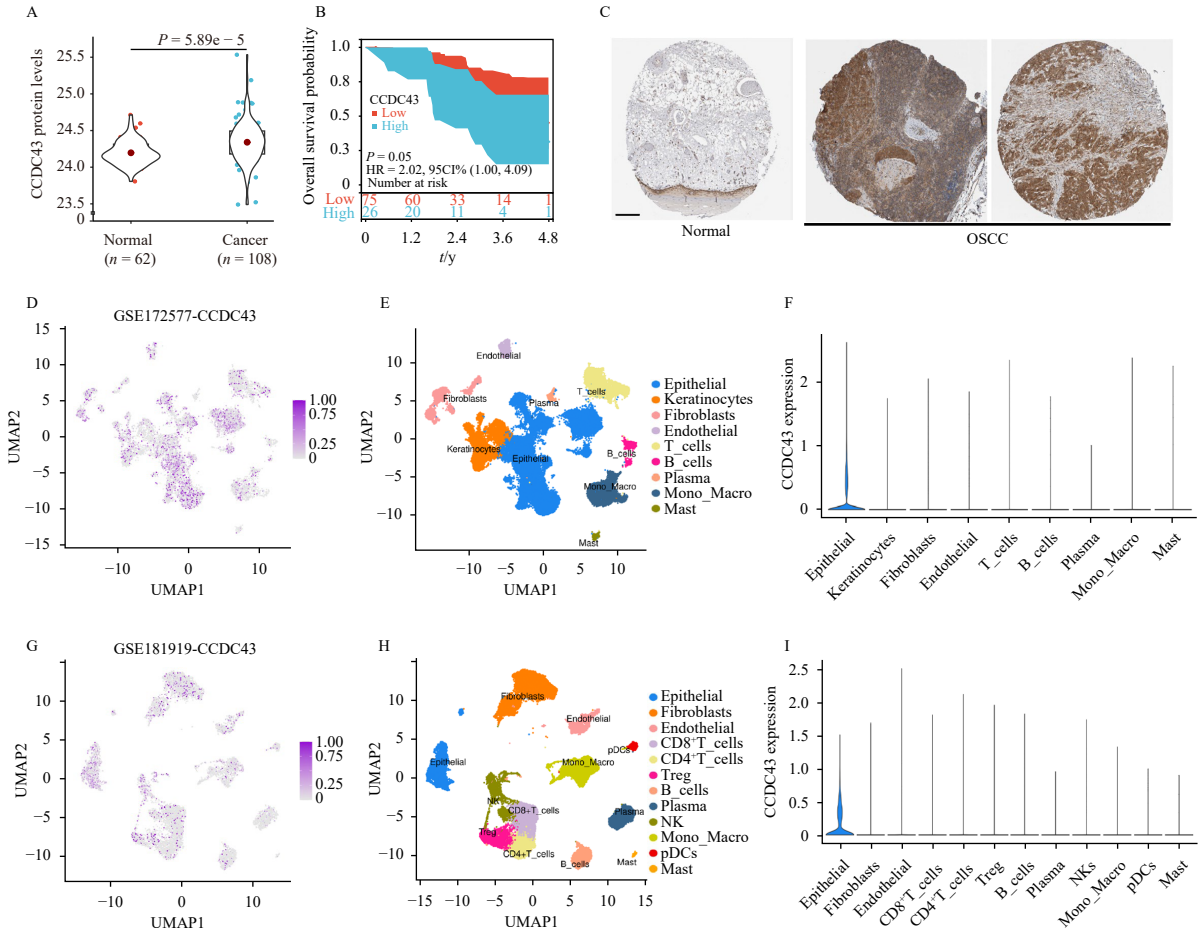


Fig. 3 CCDC43 expression and clinical relevance in HNSC revealed by proteomic and single-cell transcriptomic analyses. (A) CCDC43 protein levels were upregulated in tumor tissues compared to normal controls in the CPTAC_HNSC dataset. (B) High CCDC43 protein expression correlated with shorter OS in CPTAC_HNSC. (C) CCDC43 expression was upregulated in tumor tissues compared to normal controls in the Human Protein Atlas. Scale bar: 100 μm. (D–I) CCDC43 was specifically enriched in malignant epithelial cells within the OSCC microenvironment, as shown in single-cell datasets GSE172577 (D–F) and GSE181919 (G–I).

sensitivity in OSCC by facilitating DNA repair.

3.5. CCDC43 interacted with and protected PNKP from degradation

To further elucidate the mechanism underlying CCDC43-impaired platinum sensitivity, we screened for its potential interacting proteins. Interrogation of both the IntAct (https://www.ebi.ac.uk/intact) and BioGRID (https://thebiogrid.org) databases revealed PNKP, a key repair enzyme, as the most probable interacting protein of CCDC43. Co-IP assays confirmed that CCDC43 and PNKP interacted in OSCC cells (Fig. 6A). Interestingly, CCDC43 knockdown resulted in a significant decrease in PNKP protein levels (Figs. 6B and 6C) without affecting its mRNA levels (Fig. 6D), suggesting a post-transcriptional mechanism. CHX chase assays showed that the half-life of PNKP was reduced in CCDC43-silenced cells (Figs. 6E and 6F). Since GSEA revealed that CCDC43 was enriched in the proteasome pathway (Fig. 4A), we next investigated the effect of CCDC43 on ubiquitin-proteasome pathway-mediated PNKP degradation. Furthermore, Co-IP assays revealed that CCDC43 silencing significantly increased PNKP poly-ubiquitination, and MG-132 treatment blocked the degradation of ubiquitinated PNKP (Figs. 6G and 6H). These results indicated that CCDC43 acted as a scaffold that shielded PNKP from the ubiquitination and degradation.

3.6. Neferine targeted the CCDC43-PNKP interface to trigger PNKP degradation

Using protein-protein docking, we identified a high-affinity interaction between CCDC43 and PNKP (binding energy = −16.5 kcal·mol^{-1}) (Fig. 7A, Table S4). We then applied artificial intelligence-based virtual screening using the HelixVS platform to recognize natural compounds as potential PPI inhibitors (Table S5). Neferine was calculated to dock with PNKP, exhibiting a binding

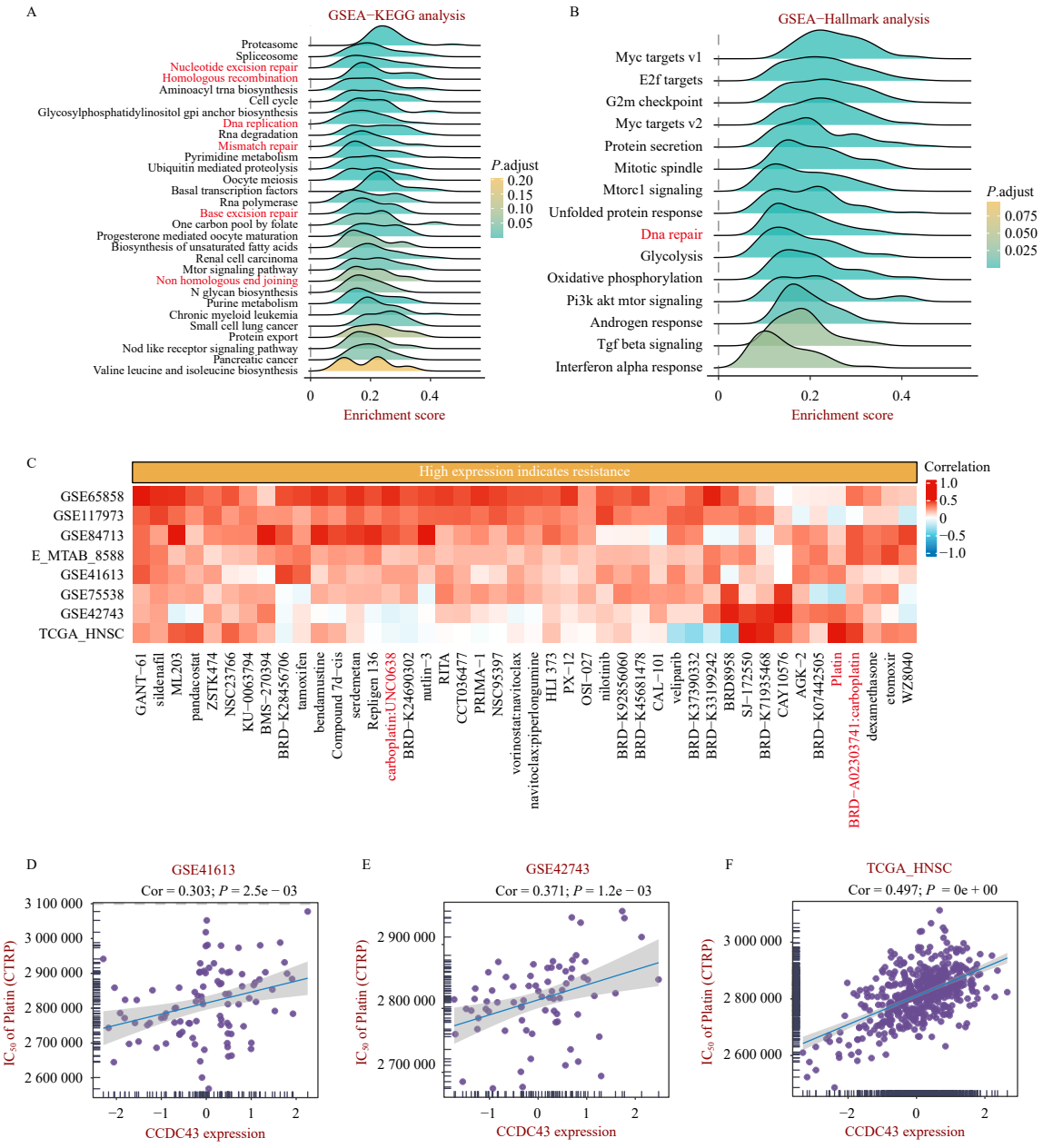


Fig. 4 Bioinformatics analyses across multiple HNSC cohorts implicated the involvement of CCDC43 in DNA repair and platinum resistance. (A) KEGG analysis revealed positive correlations between CCDC43 expression and DNA repair pathways and DNA replication. (B) HALLMARK analysis showed a positive correlation between CCDC43 expression and DNA repair. (C) Heatmap displaying positive correlations between CCDC43 expression and platinum resistance across multiple HNSC datasets. (D-F) CCDC43 expression positively correlated with cisplatin IC50 in GSE41613 (D), GSE42743 (E), and TCGA_HNSC (F).

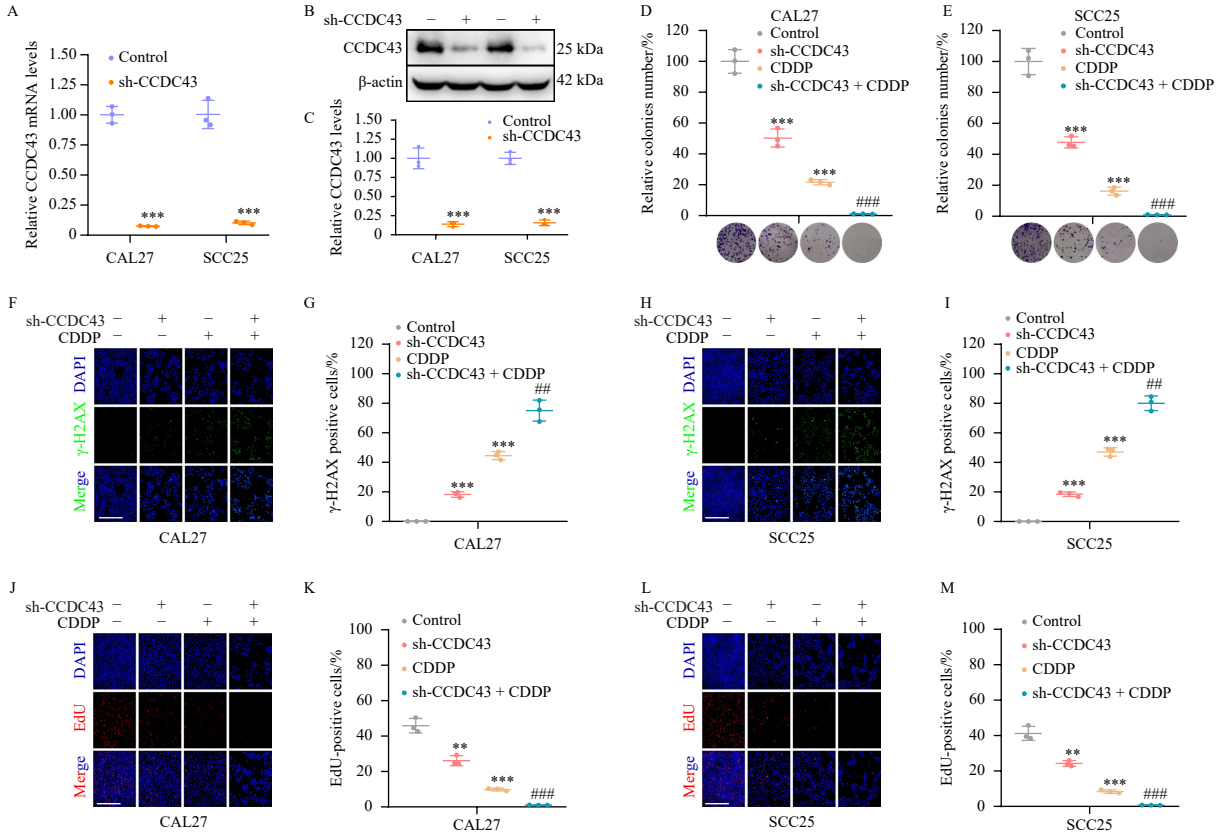
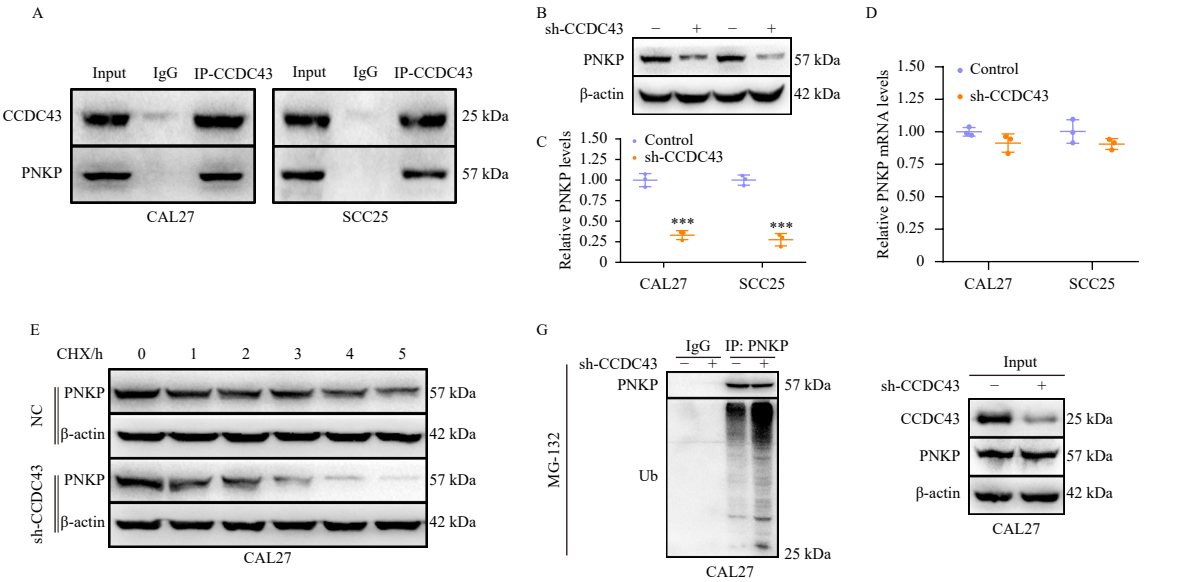


Fig. 5 CCDC43 promoted DNA damage repair and platinum resistance in OSCC. (A–C) Knockdown efficiency of CCDC43 in CAL27 and SCC25 cells confirmed by qPCR (A) and western blotting (B, C). (D, E) Colony formation assays showed that CCDC43 knockdown enhanced cisplatin sensitivity in CAL27 (D) and SCC25 (E) cells. (F–I) Immunofluorescence staining showed that CCDC43 knockdown promoted cisplatin-induced DNA damage in CAL27 (F, G) and SCC25 (H, I) cells. (J–M) EdU assays showed that CCDC43 knockdown enhanced cisplatin-induced replication inhibition in CAL27 (J, K) and SCC25 (L, M) cells. $n = 3$. Scale bars: 20 μm. ** $P < 0.01$ and *** $P < 0.001$ *vs* the control group. $^{\#\#}P < 0.01$ and $^{\#\#\#}P < 0.001$ *vs* the CDDP group.

energy of -8.4 kcal·mol^{-1} (Fig. 7B). CETSA assays confirmed that neferine treatment increased the thermal stability of PNKP, indicating direct target engagement (Figs. 7C and 7D). Furthermore, treating OSCC cells with neferine suppressed PNKP expression without altering CCDC43 expression (Figs. 7E and 7F). Interestingly, comparison of the protein-protein (CCDC43-PNKP) and protein-ligand (PNKP-neferine) interactions revealed that the neferine binding site on PNKP spatially overlapped with the CCDC43-PNKP interaction interface, involving residues R396, P473, and S475 of PNKP (Fig. 7B, Table S4). Crucially, Co-IP assays showed that neferine treatment disrupted the interaction between CCDC43 and PNKP (Figs. 7G and 7H). This disruption was accompanied by a significant increase in PNKP ubiquitination, while CCDC43 overexpression reversed this effect (Figs. 7I and 7J).

3.7. Neferine enhanced cisplatin sensitivity to suppress OSCC growth

Neferine exhibited moderate cytotoxicity as a monotherapy (Figs. S2A and B) and improved cisplatin sensitivity in colony formation assays (Figs. 8A and 8B). The combination treatment induced massive DNA damage, as evidenced by intense γ-H2AX



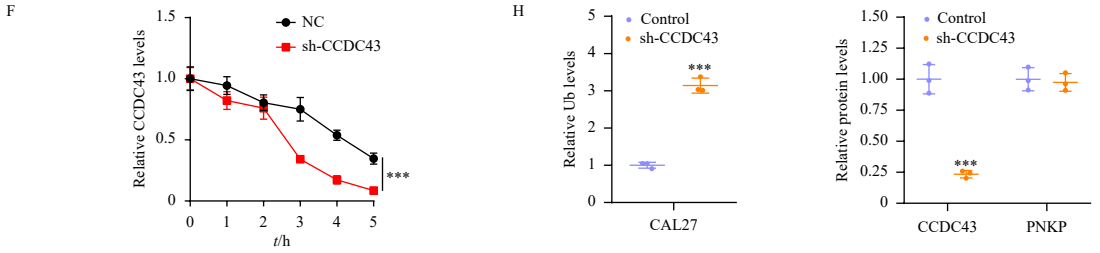


Fig. 6 CCDC43 interacted with PNKP to promote its ubiquitin-mediated degradation. (A) Co-IP confirmed the interaction between CCDC43 and PNKP in CAL27 and SCC25 cells. (B–D) Effect of CCDC43 knockdown on PNKP protein (B, C) and mRNA (D) levels in CAL27 and SCC25 cells. (E, F) CHX chase assays showed that CCDC43 knockdown shortened the half-life of PNKP protein. (G, H) Co-IP assays showed that CCDC43 knockdown facilitated PNKP ubiquitination in MG-132-treated CAL27 cells. CCDC43-silenced and control CAL27 cells were treated with MG-132 (10 μmol·L^{-1}, 8 h) prior to harvest for Co-IP assays. $n = 3$. *** $P < 0.001$ *vs* the control group.

staining (Figs. 8C–8F). Furthermore, EdU incorporation assays revealed that neferine augmented the suppressive effect of cisplatin on DNA replication (Figs. 8G–8J), phenocopying CCDC43 knockdown. In the CAL27 xenograft model, the combination of neferine and cisplatin resulted in profound tumor regression (Figs. 8K–8M). Assessment of neferine toxicity *in vivo* revealed

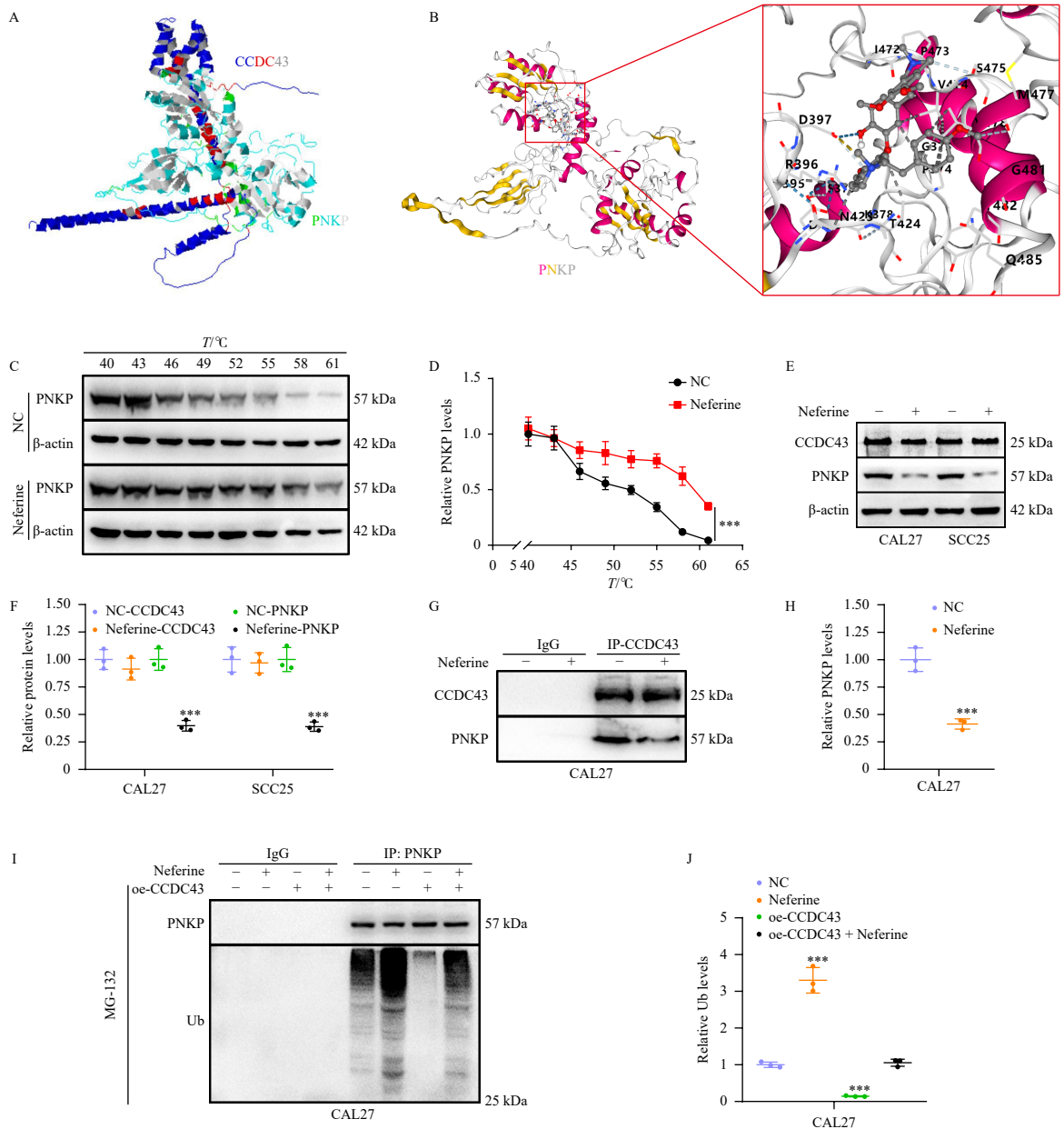


Fig. 7 Neferine disrupted the CCDC43-PNKP interaction and promoted PNKP ubiquitination. (A) Protein-protein docking revealed the predicted interaction interface between CCDC43 and PNKP. (B) Molecular docking showed the predicted binding of neferine to PNKP and the key residues involved. (C, D) CETSA showed the effect of neferine on PNKP protein stability. (E, F) Western blot analysis of CCDC43 and PNKP expression in CAL27 and SCC25 cells treated with neferine. (G, H) Co-IP assays showed that neferine disrupted the CCDC43-PNKP interaction. (I, J) Co-IP assays showed the effect of neferine on CCDC43-mediated PNKP ubiquitination in MG-132-treated CAL27 cells. CCDC43-overexpressing and control CAL27 cells were treated with neferine (40 μmol·L^{-1}, 48 h) and then MG-132 (10 μmol·L^{-1}, 8 h) prior to harvest for Co-IP assays. $n = 3$. *** $P < 0.001$ *vs* the control group.

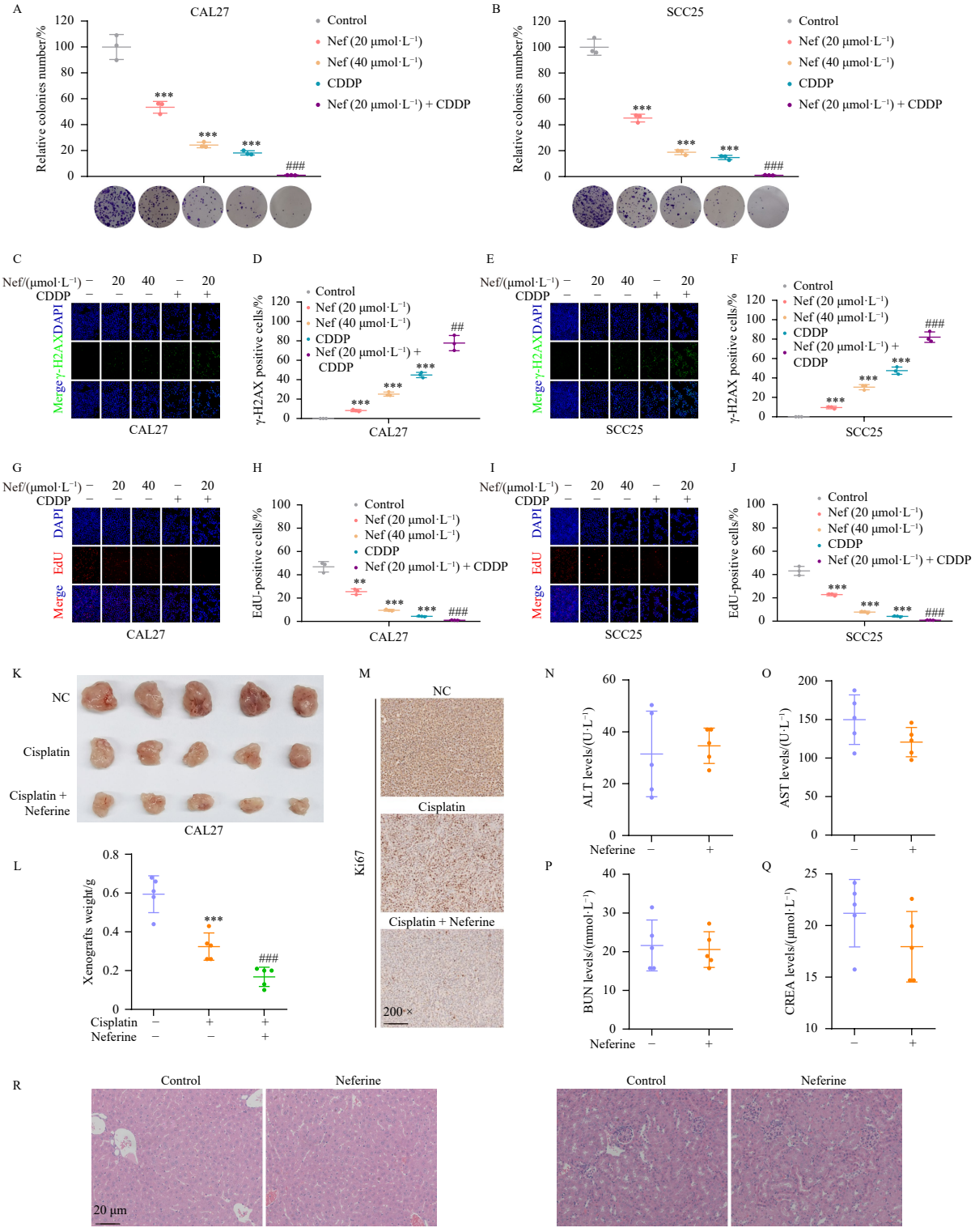


Fig. 8 Neferine impaired DNA damage repair and enhanced platinum sensitivity in OSCC. (A, B) Colony formation assays showed that neferine enhanced cisplatin sensitivity in CAL27 (A) and SCC25 (B) cells. $n = 3$. (C–F) Immunofluorescence staining showed that neferine promoted cisplatin-induced DNA damage in CAL27 (C, D) and SCC25 (E, F) cells. $n = 3$. (G–J) EdU assays showed that neferine enhanced cisplatin-induced replication inhibition in CAL27 (G, H) and SCC25 (I, J) cells. $n = 3$. (K, L) *In vivo* xenograft studies demonstrated that neferine enhanced cisplatin sensitivity. $n = 5$. (M) Representative immunohistochemical images (200 ×) of xenografts showing Ki67 expression. (N–Q) *In vivo* toxicity assessment: serum ALT (N), AST (O), BUN (P), and CREA (Q) levels in mice treated with or without neferine. $n = 5$. (R) Representative H&E staining images of liver and kidney sections from control and neferine-treated mice. $n = 5$. Scale bars: 20 μm. ** $P < 0.01$ and *** $P < 0.001$ *vs* the control group. ## $P < 0.01$ and ### $P < 0.001$ *vs* the CDDP group.

that serum markers (ALT, AST, BUN, CREA) remained within normal ranges (Figs. 8N–8Q). ine, a bioactive alkaloid from *Nelumbo nucifera Gaertn.*, effectively disrupted this axis, thereby sensitizing OSCC Additional H&E staining of the liver and kidney from treated mice revealed no histopathological abnormalities, indicating that neferine did not cause acute toxicity (Fig. 8R).

4. Discussion

Despite advances in OSCC treatment, chemoresistance remains a major clinical hurdle, underscoring the critical need to move beyond traditional cytotoxic mechanisms [26]. Our study identified the CCDC43-PNKP interaction as a critical node in the DNA damage response network that impaired cisplatin sensitiv-

ity. By integrating machine learning-based target discovery, multi-omics analysis, and ethnopharmacological validation, we demonstrated that nefercells to platinum-based therapy.

Previous bioinformatics analyses revealed that CCDC43 was upregulated in advanced OSCC, where it served as an independent prognostic factor for poor survival, promoted metastasis, and impaired antitumor immunity [27]. Consistently, our work confirmed the prognostic value of CCDC43 in OSCC based on multi-omics analysis, positioning it as a promising therapeutic target. Furthermore, its specific enrichment in OSCC epithelial cells, as revealed by single-cell analysis, underscores its role as a cell-intrinsic driver of the malignant phenotype. Scaffold proteins, despite lacking intrinsic enzymatic activity, are the master architects of cellular signaling [28]. Our findings elevated CCDC43 from a mere structural protein to a pivotal regulator of the DNA damage response in OSCC. CCDC proteins are characterized by a versatile structural motif in which two to six α-helices coil together like rope strands, providing a stable platform for multi-protein complex assembly [29]. In the context of cancer, many CCDC proteins have been found to be hijacked to stabilize oncogenic signaling [30]. Previous studies reported that CCDC43 interacted with YY1 and FHL1 in gastric cancer [18, 19]. Consistently, our work proposed that CCDC43 functioned as a stabilizer for PNKP. PNKP could repair cisplatin-damaged DNA by restoring termini to a ligation-competent 3'-hydroxyl and 5'-phosphate state [31]. DNA lesions that block the progression of replication forks activate checkpoint pathways to temporarily arrest S-phase progression and facilitate repair, thereby inhibiting DNA synthesis until the damage is resolved [32]. Our data suggested that CCDC43 bound to PNKP, shielding it from ubiquitination and degradation [33]. thereby impairing cisplatin sensitivity by regulating the DNA damage response. Thus, CCDC43 could serve as a biomarker for predicting poor response to standard cisplatin therapy.

Advances in rational design, computational methods, and screening technologies have enabled the targeting of protein-protein interactions, transforming them from traditionally undruggable targets into a tractable class for therapeutic intervention [34]. A key advance of our study was the identification of neferine as a potent inhibitor of the CCDC43-PNKP interaction through AI-based VS. Unlike conventional structure-based or ligand-based methods that rely on physics-based docking and scoring functions, AI-based VS integrates advanced algorithms such as graph neural networks, transformers, and convolutional neural networks to learn complex patterns from molecular data [35]. AI-based methods are particularly valuable for challenging targets such as protein-protein interactions, where traditional docking often struggles due to flat, featureless interfaces [36]. Neferine possesses a unique bisbenzylisoquinoline structure. This structural feature provides the molecular complexity and hydrophobicity required for intercalation into the protein-protein interface [37]. Consistent with previous reports, our molecular docking and CETSA results provided a structural rationale for this activity, showing that neferine targeted the PNKP interface required for CCDC43 binding. By occupying this interface, neferine induced a conformational shift that exposed PNKP to the cellular ubiquitination machinery.

The traditional use of Nelumbo nucifera embryos for "heat-toxin" conditions, a Traditional Chinese Medicine term encompassing inflammation, hyperproliferation, and treatment resistance, provides a strong ethnopharmacological foundation for this study, as these features are hallmarks of advanced OSCC [8]. Our molecular findings provided a modern scientific translation for these concepts. Furthermore, the synergy between neferine and cisplatin exemplified a beneficial herb-drug interaction that enhanced therapeutic outcomes [38]. Cisplatin exerted its anticancer effect by damaging DNA, whereas neferine sensitized cells by blocking DNA repair. This combination presented a dose-sparing strategy to circumvent the dose-limiting toxicities of cisplatin. In traditional practice, Lian Zi Xin is considered to have a "cold" nature, which, according to Traditional Chinese Medicine principles, renders it suitable for treating "heat" conditions without causing excessive harm. This aligns with our animal data, which demonstrated that neferine treatment exhibited no significant acute toxicity. Furthermore, neferine may exert protective effects by mitigating the systemic oxidative stress induced by high-dose platinum therapy [9, 39], supporting its potential as a "heat-toxin-moderating" adjunct to platinum-based chemotherapy. Given its excellent efficacy [9, 40], developing synthetic derivatives of neferine with optimized pharmacokinetics and enhanced binding affinity for the CCDC43-PNKP interface represents a promising avenue for drug development. Future studies could include thermal proteome profiling, drug affinity responsive target stability-western blotting to assess neferine-PNKP binding, or chemoproteomic approaches to map the interactome of neferine and evaluate its selectivity. Moreover, structure-activity relationship studies may guide the development of neferine derivatives with improved binding affinity and fewer off-target effects. Unbiased affinity purification-mass spectrometry would also be valuable for characterizing the CCDC43 interactome in OSCC. Chronic toxicity evaluation with multiple dose levels and additional endpoints would be beneficial to further assess the long-term safety profile of neferine for clinical translation. In addition, autophagy inhibitors could help clarify the degradation pathways regulating PNKP stability, and quantitative biophysical assays such as surface plasmon resonance or microscale thermophoresis would be useful to determine the binding affinity and kinetics of the neferine-PNKP interaction. Finally, we acknowledge that the absence of a neferine monotherapy group in the present *in vivo* study limits our ability to quantify the synergistic contribution of neferine relative to its additive antitumor effects.

5. Conclusion

This study provided a comprehensive molecular characterization of the CCDC43-PNKP axis, identifying it as a critical target for enhancing cisplatin sensitivity in OSCC. Through a multidisciplinary approach, we demonstrated that CCDC43 functioned as a scaffold, shielding PNKP from ubiquitin-mediated degradation to enhance DNA repair and impair cisplatin sensitivity. Crucially, we identified neferine as a potential inhibitor of the CCDC43-PNKP interaction (Fig. 9). By disrupting this complex,

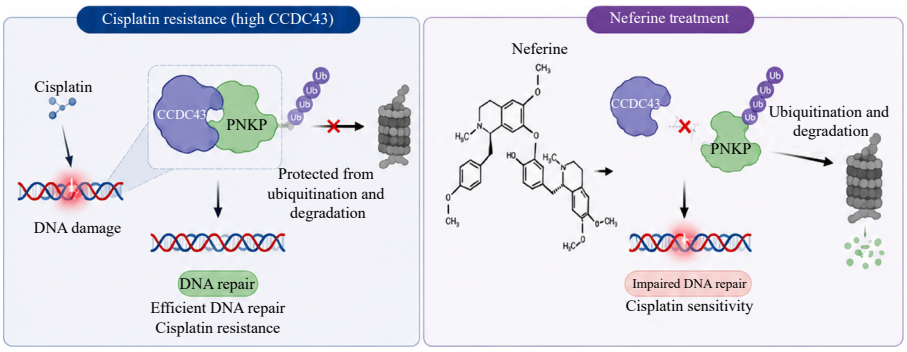


Fig. 9 Working model of neferine disrupting the CCDC43-PNKP interaction to regulate DNA damage repair and platinum sensitivity in OSCC.

neferine induced PNKP degradation, sensitizing OSCC cells to cisplatin and driving significant tumor regression with a favorable safety profile *in vivo*. This work establishes CCDC43 as a novel target within the DNA damage response network and provides modern scientific validation for neferine, offering a promising and targeted strategy to overcome chemoresistance in OSCC.

Funding

This work was supported by the Foreign Cooperation Project of Fujian Provincial Department of Science and Technology (No. 2026I0006), the Open Research Project of Key Laboratory of Radiation Biology of Fujian higher education institutions (No. 2023FSSW-02), and Fujian Provincial Finance Project (No. BPB-2023ZXF).

Data availability

The datasets used and/or analyzed during this study are available from the corresponding author on reasonable request.

Declaration of competing interest

The authors declare no conflict of interest.

References

1 Rumgay H, Colombet M, Ramos da Cunha A, et al. Global incidence of lip, oral cavity, and pharyngeal cancers by subsite in 2022. *CA Cancer J Clin*. 2026;1-13. https://doi.org/10.3322/caac.70048.
2 Collaborators GBDC. The global, regional, and national burden of cancer, 1990-2023, with forecasts to 2050: a systematic analysis for the Global Burden of Disease Study 2023. *Lancet*. 2025;406(10512):1565-1586. https://doi.org/10.1016/S0140-6736(25)01635-6.
3 Xue NN, Wang Y, Wang ZY, et al. Trends in immunotherapy for oral squamous cell carcinoma. *Cell Oncol (Dordr)*. 2025;48(5):1159-1179. https://doi.org/10.1007/s13402-025-01068-3.
4 Cascardi E, Della Mura M, Sgarro N, et al. Chorus line in oral squamous cell carcinoma: how stromal and immune players orchestrate tumor progression (Review). *Int J Mol Med*. 2026;57(4):90. https://doi.org/10.3892/ijmm.2026.5761.
5 Zhou FY, Waterman DP, Ashton M, et al. Prolonged cell cycle arrest in response to DNA damage in yeast requires the maintenance of DNA damage signaling and the spindle assembly checkpoint. *eLife*. 2024;13:RP94334. https://doi.org/10.7554/eLife.94334.
6 Cecati M, Pozzi V, Pompei V, et al. Cisplatin as a xenobiotic agent: molecular mechanisms of actions and clinical applications in oncology. *J Xenobiot*. 2026;16(1):9. https://doi.org/10.3390/jox16010009.
7 Lin X, Wang F, Chen J, et al. N(6)-methyladenosine modification of CENPK mRNA by ZC3H13 promotes cervical cancer stemness and chemoresistance. *Mil Med Res*. 2022;9(1):19. https://doi.org/10.1186/s40779-022-00378-z.
8 Ren X, Chen H, Wang H, et al. Advances in the pharmacological effects and mechanisms of Nelumbo nucifera gaertn. *Extract nuciferine. J Ethnopharmacol*. 2024;331:118262. https://doi.org/10.1016/j.jep.2024.118262.
9 Bharathi PL, Huang CY, Hu RM, et al. An updated review on pharmacological properties of neferine-A bisbenzylisoquinoline alkaloid from Nelumbo nucifera. *J Food Biochem*. 2021;45(12):e13986. https://doi.org/10.1111/jfbc.13986.
10 Wang XJ, Li B, Gao JY, et al. The OGG1 Ser326Cys polymorphism: molecular mechanisms of disease susceptibility and precision medicine applications. *Clin Epigenetics*. 2025;17(1):153. https://doi.org/10.1186/s13148-025-01978-x.
11 Sekeres M, Lengle D, Abbey L, et al. Epigenetic targeting of DNA damage response (DDR)-related mechanisms to overcome acquired cisplatin resistance of tumor cells. *Biochim Biophys Acta Mol Cell Res*. 2025;1872(7):120018. https://doi.org/10.1016/j.bbamcr.2025.120018.
12 Gohil D, Sarker AH, Roy R. Base excision repair: mechanisms and impact in biology, disease, and medicine. *Int J Mol Sci*. 2023;24(18):14186. https://doi.org/10.3390/ijms241814186.
13 Carter J, Hulse M, Sivakumar M, et al. PRMT5 inhibitors regulate DNA damage repair pathways in cancer cells and improve response to PARP inhibition and chemotherapies. *Cancer Res Commun*. 2023;3(11):2233-2243. https://doi.org/10.1158/2767-9764.CRC-23-0070.
14 Shire Z, Vakili MR, Morgan TDR, et al. Nanoencapsulation of novel inhibitors of PNKP for selective sensitization to ionizing radiation and irinotecan and induction of synthetic lethality. *Mol Pharm*. 2018;15(6):2316-2326. https://doi.org/10.1021/acs.molpharmaceut.8b00169.
15 Wang Y, Coulombe Y, Yueh WT, et al. PALB2 and 53BP1 govern post-resection homologous recombination DNA repair. *Mol Cell*. 2025;85(15):2824-2838. https://doi.org/10.1016/j.molcel.2025.07.003.
16 Okano T, Takata M, Fujita M, et al. Recent advances in understanding the molecular mechanisms of SLX4 recruitment in the replication stress response. *DNA Repair (Amst)*. 2025;156:103911. https://doi.org/10.1016/j.dnarep.2025.103911.
17 Liu Z, Yan WW, Liu SH, et al. Regulatory network and targeted interventions for CCDC family in tumor pathogenesis. *Cancer Lett*. 2023;565:216225. https://doi.org/10.1016/j.canlet.2023.216225.
18 Wang J, Wu X, Dai W, et al. The CCDC43-ADRM1 axis regulated by YY1, promotes proliferation and metastasis of gastric cancer. *Cancer Lett*. 2020;482:90-101. https://doi.org/10.1016/j.canlet.2020.03.026.
19 Chen Y, Pei M, Li J, et al. Disruption of the CCDC43-FHL1 interaction triggers apoptosis in gastric cancer cells. *Exp Cell Res*. 2022;415(1):113107. https://doi.org/10.1016/j.yexcr.2022.113107.
20 Wang J, Liu G, Liu M, et al. The FOXK1-CCDC43 axis promotes the invasion and metastasis of colorectal cancer cells. *Cell Physiol Biochem*. 2018;51(6):2547-2563. https://doi.org/10.1159/000495924.
21 Lin Y, Chen X, Lin L, et al. Sesamolin serves as an MYH14 inhibitor to sensitize endometrial cancer to chemotherapy and endocrine therapy *via* suppressing MYH9/GSK3beta/beta-catenin signaling. *Cell Mol Biol Lett*. 2024;29(1):63. https://doi.org/10.1186/s11658-024-00583-9.
22 Lin X, Liu J, Zou Y, et al. Xanthotoxol suppresses non-small cell lung cancer progression and might improve patients' prognosis. *Phytomedicine*. 2022;105:154364. https://doi.org/10.1016/j.phymed.2022.154364.
23 Lin X, Chen D, Chu X, et al. Oxypalmatine regulates proliferation and apoptosis of breast cancer cells by inhibiting PI3K/AKT signaling and its efficacy against breast cancer organoids. *Phytomedicine*. 2023;114:154752. https://doi.org/10.1016/j.phymed.2023.154752.
24 Lin X, Lin T, Wang X, et al. Sesamol serves as a p53 stabilizer to relieve rheumatoid arthritis progression and inhibits the growth of synovial organoids. *Phytomedicine*. 2023;121:155109. https://doi.org/10.1016/j.phymed.2023.155109.
25 Lin X, Chen J, Tao C, et al. Osthole regulates N6-methyladenosine-modified TGM2 to inhibit the progression of rheumatoid arthritis and associated interstitial lung disease. *Med Comm*. 2023;4(2):e219. https://doi.org/10.1002/mco2.219.
26 Zhou Y, Wang L, Liu M, et al. Oral squamous cell carcinoma: insights into cellular heterogeneity, drug resistance, and evolutionary trajectories. *Cell Biol Toxicol*. 2025;41(1):101. https://doi.org/10.1007/s10565-025-10048-0.
27 Wang Z, Zhang H, Zhai Y, et al. Single-cell profiling reveals heterogeneity of primary and lymph node metastatic tumors and immune cell populations and discovers important prognostic significance of CCDC43 in oral squamous cell carcinoma. *Front Immunol*. 2022;13:843322. https://doi.org/10.3389/fimmu.2022.843322.
28 Ball NJ, Barnett SFH, Goult BT. Mechanically operated signalling scaffolds. *Biochem Soc Trans*. 2024;52(2):517-527. https://doi.org/10.1042/BST20221194.
29 Priyanka PP, Yenugu S. Coiled-coil domain-containing (CCDC) proteins: functional roles in general and male reproductive physiology. *Reprod Sci*. 2021;28(10):2725-2734. https://doi.org/10.1007/s43032-021-00595-2.
30 Shen H, Li H, Tang H. CCDC110 promotes the progression of hepatocellular carcinoma by activating the TGF-beta/SMAD signaling pathway through targeted regulation of TGFBR1. *Cancer Cell Int*. 2025;25(1):183. https://doi.org/10.1186/s12935-025-03803-0.
31 Boccard SG, Marand SV, Geraci S, et al. Inhibition of DNA-repair genes Ercc1 and Mgmt enhances temozolomide efficacy in gliomas treatment: a pre-clinical study. *Oncotarget*. 2015;6(30):29456-68. https://doi.org/10.18632/oncotarget.4909.
32 Yates LA, Zhang X, Burgers PM. DNA damage and replication stress checkpoints. *Annu Rev Biochem*. 2025;94(1):195-221. https://doi.org/10.1146/annurev-biochem-072324-031915.
33 Morozko EL, Smith-Geater C, Monteys AM, et al. PIAS1 modulates striatal transcription, DNA damage repair, and SUMOylation with relevance to Huntington's disease. *Proc Natl Acad Sci U S A*. 2021;118(4):e2021836118. https://doi.org/10.1073/pnas.2021836118.
34 Hong SH, Nguyen T, Ongkingco JF, et al. From concepts to inhibitors: a blueprint for targeting protein-protein interactions. *Chem Rev*. 2025;125(14):6819-6869. https://doi.org/10.1021/acs.chemrev.5c00046.
35 Manan A, Baek E, Ilyas S, et al. Digital alchemy: the rise of machine and deep learning in small-molecule drug discovery. *Int J Mol Sci*. 2025;26(14):6807. https://doi.org/10.3390/ijms26146807.
36 Szalai TV, Peczka N, Sipos-Szabo L, et al. Ultrahigh-throughput virtual screening strategies against PPI targets: a case study of STAT inhibitors. *J Chem Inf Model*. 2025;65(14):7734-7748. https://doi.org/10.1021/acs.jcim.5c00907.
37 Xie B, Tian LW, Liu C, et al. Disruption of the eEF1A1/ARID3A/PKC-delta complex by Neferine inhibits macrophage glycolytic reprogramming in atherosclerosis. *Adv Sci (Weinh)*. 2025;12(15):e2416158. https://doi.org/10.1002/advs.202416158.
38 Manogaran P, Somasundaram B, Viswanadha VP. Reversal of cisplatin resistance by neferine/isoliensinine and their combinatorial regimens with cisplatin-induced apoptosis in cisplatin-resistant colon cancer stem cells (CSCs). *J Biochem Mol Toxicol*. 2022;36(3):e22967. https://doi.org/10.1002/jbt.22967.
39 Li H, Ge H, Song X, et al. Neferine mitigates cisplatin-induced acute kidney injury in mice by regulating autophagy and apoptosis. *Clin Exp Nephrol*. 2023;27(2):122-131. https://doi.org/10.1007/s10157-022-02292-z.
40 Liu Y, Wang C, Liao Q, et al. Pharmacological potential and mechanisms of bisbenzylisoquinoline alkaloids from lotus seed embryos. *Biomolecules*. 2025;15(10):1377. https://doi.org/10.3390/biom15101377.